Inorganica Chimica Acta 487 (2019) 128–137

Contents lists available at ScienceDirect

Inorganica Chimica Acta

journal homepage: www.elsevier.com/locate/ica

Research paper

Supramolecular self-assembly, DNA interaction, antibacterial and cell viability studies of Cu(II) and Ni(II) complexes derived from NNN donor Schiff base ligand

Kalyanmoy Jana[a], Somnath Das[b], Horst Puschmann[c], Subhas Chandra Debnath[a], Aparna Shukla[d], Arun K. Mahanta[d], Maidul Hossain[b,*], Tithi Maity[e,*], Bidhan Chandra Samanta[f,*]

[a] Department of Chemistry, University of Kalyani, West Bengal, India
[b] Department of Chemistry and Chemical Technology, Vidyasagar University, Paschim Medinipur-721302, West Bengal, India
[c] Department of Chemistry, Durham University, Durham DH1 3LE, United Kingdom
[d] School of Materials Science and Technology (SMST), Indian Institute Of Technology (IIT), BHU, India
[e] Department of Chemistry, Prabhat Kumar College, Contai, Purba Medinipur-721401, West Bengal, India
[f] Department of Chemistry, Mugberia Gangadhar Mahavidyalaya, Bhupatinagar, Purba Medinipur-721425, West Bengal, India

ARTICLE INFO

Keywords:
X-ray crystallography
Antibacterial properties
DNA binding
Cu(II) and Ni(II) complexes

ABSTRACT

In the present study, synthesis of two complexes, namely $[Cu(L)Cl_2]$ (1) and $[Ni(L)Cl(H_2O)_2)]Cl$ (2), where L = piperidin-2-yl-N-(1-(pyridin-2-yl) ethylidene)methanamine were reported along with their characterization by spectroscopic techniques. The crystal structures were elucidated by single crystal X-ray diffraction technique. The structures of the complexes showed square pyramidal geometry for Cu(II) and octahedral geometry for Ni(II) centers. Different characterization techniques including electronic absorption spectroscopy, viscosity measurements and fluorescence spectroscopy were used to study the binding interaction of complex 1 and 2 with Calf thymus DNA (CT-DNA). The result reflected that both the complexes were able to exhibit DNA binding potential by intercalation pathway. Study of antibacterial activity using the bacterial strain E. coli showed that only complex 1 exhibited antibacterial property. Besides, metal, ligand and its complexes were evaluated individually for cell viability studies through MTT assay of HeLa cells. It is observed that cell viability increases with time for all the systems illustrating biocompatible nature of metals, ligands and their complexes. Among the complexes 1 and 2, complex 1 is suitable for higher cell viability.

1. Introduction

There are huge applications of transition metal complexes in the vast areas of materials science to biological sciences. This attracts the chemists very much to be interested in this field. In the last decade a greater interest had been observed for transition metal complexes of Schiff bases due to their anti-inflammatory, anti-carcinogenic, anti-pyretic, anti-diabetic, anti-bacterial and antifungal properties [1–8]. Besides, opportunities to enhance the solubility, inducing substrate chirality, tuning the metal centered electronic factor and also the stability of either homogeneous or heterogeneous catalysts are offered by Schiff bases [9–11]. Complexes derived from Schiff bases are the most widely studied coordination compounds in the past few years, because they are now increasingly used as biochemical, analytical and anti-microbial reagents [12–14]. It has also been found that among tridentate and bidentate Schiff base ligands, the tridentate Schiff base ligands are more suitable ligand systems for stabilizing organo-metal complexes due to having additional donor atom for coordination. Actually the various factors control the coordination geometry of these complexes. Among these factors the size and electronic configuration of the central metal ions, non-bonding interactions between atoms in different ligand arms and the inherent rigidity due to the presence of aromatic rings are very much important. Self-assembly via weak interaction has been projected as a useful and powerful protocol to construct the predesigned and well-defined architectures. Molecular self-assembly which is at the heart of crystalline molecular materials can be constructed through various forces such as hydrogen bonding, C—H—π and π—π interactive forces [15–20]. For directing molecular self-assembly, the key factors which are essential are identification and control of recognition among a set of molecular building blocks. In this context, the hydrogen bonding which is of primary importance in molecular recognition has been utilized extensively in the design of

* Corresponding authors.
E-mail address: hossainm@mail.vidyasagar.ac (B.C. Samanta).

https://doi.org/10.1016/j.ica.2018.12.007
Received 3 May 2018; Received in revised form 29 October 2018; Accepted 4 December 2018
Available online 05 December 2018
0020-1693/

functional materials.

Besides, the DNA interaction of Schiff base metal complexes has also gained much interest towards their applications in biotechnology and medicine. The scientific community has showed that metal coordination compounds have shown some outstanding DNA-binding and cleavage properties, as well as antibacterial activities [21–25]. It is seen that transition metals are particularly suitable for this purpose, because they can adopt a wide variety of oxidation states, coordination numbers and geometries, in comparison to other main group elements. So, over the past decades, considerable interest in the synthesis and characterization of transition metal complexes with Schiff Base ligands had been developed to check the role of metal active sites in several catalytic biological processes.

In the present study, the synthesis and characterization of two mono-nuclear Cu(II) and Ni(II) complexes derived from a tridentate Schiff base ligand has been reported. Crystal structures of those complexes have been detected by X-ray diffraction method and molecular recognition has been done involving mainly hydrogen bonding interaction. Besides, the potential CT-DNA interactions and antibacterial behavior of the complexes 1 and 2 have been examined. Several techniques including electronic absorption titration, viscosity measurements and fluorescence spectroscopy have been employed to monitor their prospective binding interaction with CT-DNA. Their antimicrobial properties against *E. coli* and cell viability studies have also been determined through the agar-well diffusion method and MTT assay of HeLa cells respectively.

2. Material and method section

2.1. Materials

All the chemicals which were used in this work were of reagent grade and used without purifying them. 2-acyl pyridine, methanol, $NiCl_2{\cdot}6H_2O$ and $CuCl_2{\cdot}2H_2O$ were purchased from Merck. CT-DNA and Ethidium Bromide (EB) were obtained from Sigma-Aldrich Chemicals Co., (St. Louis, MO, USA). CT-DNA concentration and EB concentration were measured photometrically on the basis of molar extinction coefficient values (13,200 M^{-1} cm^{-1} at 260 nm for CT-DNA and 5000 M^{-1} cm^{-1} at 480 nm for EB); no deviation from Beers law was observed during concentration measurement.

Citrate -phosphate (CP) buffer prepared from Millipore water (10 mM [Na^+]) (pH 7.12) was used to prepare the reagent solution and also used to carry out whole interaction study. Unnecessary particulate from the buffer solutions was removed by passing the whole buffer solution through 0.45 μm (Millipore India Pvt. Ltd., Bangalore, India) filter paper (repeated two times) and prior to use the solution was stored in 4 °C.

2.2. Synthesis of ligand L

The Schiff base ligand L was prepared from the reaction of 2-acyl pyridine (1.21 g, 10 mmol) and piperidine-2-yl-methylamine (1.14 g, 10 mmol) in MeOH solvent (35 ml) by refluxing the mixture for 3 h. A change in color was observed but no precipitate was obtained. Then the solvent was evaporated and a gummy mass was obtained (Scheme 1). This crude product was then used directly for the preparation of the complexes.

2.3. Synthesis of [Cu(L)Cl_2] (1)

To synthesize the complex 1 a solution of $CuCl_2{\cdot}2H_2O$ (0.170 g, 1 mmol) in MeOH (10 ml) was added to a stirred raw tea color solution of L (0.203 g, 1 mmol) in MeOH (15 ml) and the mixture was then refluxed in air for 3 h. It resulted to a green color solution. The solution was filtered and kept for slow evaporation. Single crystals of the complex suitable for X-ray crystallography were obtained after 1 month from the solution.

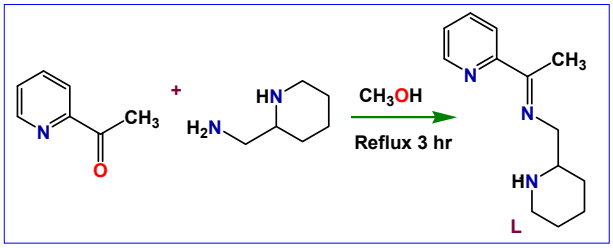

Scheme 1. Synthetic pathway for ligand L.

Yield: 0.25 g (67%). Anal. Calc. for $C_{13}H_{19.4}Cl_2CuN_3O_{0.2}$: C, 43.94; H, 5.35; N, 11.83.Found: C, 43.8; H, 5.2; N, 11.80. Selected FTIR bands (KBr, cm^{-1}; s = strong, vs = very strong, m = medium, br = broad): 3437 (br), 3051 (vs), 2916 (vs), 1490 (m), 1340 (s), 1305 (m), 1666 (s), 1203 (m). UV−vis spectra [λmax, nm (ε, L mol^{-1} cm^{-1}); MeOH solution]: 285 (3041).

2.4. Synthesis of [Ni(L)Cl(H_2O)$_2$]Cl(2)

The complex 2 was synthesized from a solution of $NiCl_2{\cdot}6H_2O$ (0.130 g, 1 mmol) in MeOH (15 ml) and a stirred raw tea color solution of L (0.203 g, 1 mmol) in MeOH (15 ml) by refluxing the mixture in air for 3 h. A deep pink color solution was resulted at the completion of the reaction. The solution was then filtered and single crystals of the complex suitable for X-ray crystallography were obtained after 1 month from the solution through slow evaporation.

Yield: 0.21 g (63%). Anal. Calc. for $C_{13}H_{23}Cl_2N_3NiO_2$: C, 40.73; H, 6.00; N, 10.96.Found: C, 40.65; H, 6.01; N, 10.90. Selected FTIR bands (KBr, cm^{-1}; s = strong, vs = very strong, m = medium, br = broad): 3502 (br) 3435 (br), 3053 (vs), 2918 (vs), 1489 (m), 1342 (s), 1307 (m), 1664 (s), 1205 (m).UV − vis spectra [λmax, nm (ε, L mol^{-1} cm^{-1}); MeOH solution]: 278 (9 1 7).

2.5. Physical measurements

Elemental analyses (C, H and N) were carried out on a Perkin Elmer 2400II elemental analyzer. FTIR spectroscopic analyses were done from neat samples between KBr discs on a Perkin Elmer 883 spectrometer. Electronic absorption spectra were recorded using a Systronic India UV–Vis spectrophotometer.

2.6. X-ray crystallography

A single crystal of suitable dimensions was used for data collection in a Xcalibur, Sapphire 3 diffractometer. Using Olex2 [26], the structure was solved with the Superflip [27] structure solution program for copper(II) complex and with olex2.solve [28] structure solution program for nickel(II) complex, by the Charge Flipping solution method. The model was refined with version 2016/5 of ShelXL [29] using Least Squares minimization. Cell parameters were retrieved using the Crys Alis (Pro) software and refined using Crys Alis (Pro) on 10,318 reflections, 48% of the observed reflections. Data reduction was carried out using the Crys Alis (Pro) software which corrects for Lorentz polarization. All non-hydrogen atoms were refined anisotropically. Hydrogen atom positions were determined geometrically and refined using the riding model. The locations of the heaviest atoms (Cu, Ni) were determined easily, and the O, N, and C atoms were subsequently determined from the different Fourier maps. Information regarding X-ray data collection and crystal structure refinement is summarized in Table 1 for complexes 1 & 2. Crystallographic data (excluding structure factors) have been deposited with the Cambridge Crystallographic Data Centre under the accession code CCDC1515618 & 1515614 for complexes 1 & 2 respectively.

Table 1
Crystal Parameter and Refinement Data for complex 1 and 2.

Compound reference	Complex 1	Complex 2
Formula	$C_{13}H_{19.4}Cl_2CuN_3O_{0.2}$	$C_{13}H_{23}Cl_2N_3NiO_2$
$D_{calc.}$/g cm^{-3}	1.513	1.503
μ/mm^{-1}	1.734	1.468
Formula Weight	355.35	382.95
Colour	clear light green	clear light blue
Shape	irregular	irregular
Size/mm^3	0.56 × 0.32 × 0.17	0.80 × 0.50 × 0.27
T/K	120(2)	120(2)
Crystal System	monoclinic	monoclinic
Space Group	$P2_1/n$	$P2_1/c$
a/Å	8.6528(2)	7.5010(4)
b/Å	10.6852(3)	9.4291(3)
c/Å	17.0483(4)	23.9342(9)
α/°	90	90
β/°	98.315(2)	90.033(4)
γ/°	90	90
V/Å^3	1559.66(7)	1692.81(12)
Z	4	4
Z'	1	1
Wavelength/Å	0.71073	0.71073
Radiation type	MoK_α	MoK_α
θ_{min}/°	2.819	2.715
θ_{max}/°	29.998	30.000
Measured Refl.	21,366	11,692
Independent Refl.	4551	4921
Reflections Used	4079	4128
R_{int}	0.0266	0.0341
Parameters	182	305
Restraints	0	203
Largest Peak	0.815	0.574
Deepest Hole	-0.223	-0.587
GooF	1.061	1.143
wR_2 (all data)	0.0712	0.1140
wR_2	0.0688	0.1084
R_1 (all data)	0.0307	0.0584
R_1	0.0262	0.0472
CCDC Number	1515618	1515614

2.7. Antibacterial screening

To investigate the antibacterial activity of the complex against several bacteria, the agar well diffusion method on nutrient agar medium was used with necessary modifications [30]. Antibacterial activity was studied using the bacterial strain E. coli. The bacterium under investigation was obtained from the Microbial Type Culture Collection and Gene Bank (MTCC). Agar media (broth) prepared by mixing 500 mg each of beef extract, NaCl, peptone and 3 g of agar agar in 100 ml distilled water was used. 100 μl of bacterium E. coli was added to 30 ml of broth and incubated for 24 h.

2.8. DNA interaction studies

Absorption measurement for DNA interaction studies was monitored in Shimadzu Pharmaspec 1601 unit (Shimadzu Corporation, Kyoto, Japan). A fixed concentration of 10 mM for complex **1** and 15 mM for complex **2** was used by regular adding of CT-DNA. Reference buffer solution was also incorporated with same amount of DNA to minimize the absorption of DNA during titration. The intrinsic binding constant (K) obtained from absorption titration was calculated from the following equation [31]

$$\frac{[DNA]}{(\varepsilon_a - \varepsilon_f)} = \frac{[DNA]}{(\varepsilon_b - \varepsilon_f)} + \frac{1}{K(\varepsilon_b - \varepsilon_f)} \quad (1)$$

where [DNA] is the concentration of CT-DNA in the base pairs, ε_a is the apparent absorption coefficient corresponding to A_{obs}/ [complex], ε_f is the extinction coefficient of the free complex, and ε_b is the extinction coefficient of the complex when fully bound to CT-DNA. From the plot of [DNA]/($\varepsilon_a - \varepsilon_f$) versus [DNA], K can be calculated by the ratio of the slope to intercept.

A Hitachi F7000 fluorometer (Hitachi Ltd., Tokyo, Japan) was used to study competitive fluorescence binding of the complex **1** and **2** with EB. For this study the CT DNA − EB complex was prepared first by adding 5 μM EB and 10 μM CT- DNA. Then this CT-DNA − EB complex was excited at 515 nm. The emission range was recorded at 560–700 nm followed by the regular addition of complex solution [32].

Viscosity experiments was performed in a Brookfield rotational Viscometers (Middleboro, MA 02346 U.S.A.) armed with a 1 ml LCP spindle operating at 40 rpm at 25 °C. In this experiment the viscosities of a DNA solution (1 mM) were measured in the absence and presence of increasing concentrations of the complex (0.05–0.2 mM). The relation between the relative solution viscosity (η/η_0) and DNA length (L/L_0) is given by the equation

$$L/L_0 = (\eta/\eta_0)^{1/3}$$

where L and L_0 indicate the apparent molecular length in the presence and absence of the compound respectively [33,34]. The obtained data are presented as $(\eta/\eta_0)^{1/3}$ versus r, where η denotes the viscosity of DNA in the presence of complex, and η_0 signifies the viscosity of DNA alone in buffer solution, and r represents the ratio of [complex] / [DNA].

2.9. Cell culture and maintenance

To culture HeLa (Human cervical cancer cell line) cells, Dulbecco's Modified Eagle Medium (DMEM) containing 10% heat inactivated (FBS) fetal bovine serum, 100U/ml penicillin and 100 μg/ ml streptomycin was used. Cells were incubated at 37 °C in a CO_2 incubator with 5% CO_2 supply.

2.10. Cell viability

Cell viability studies of metal, ligand and its complexes were performed through MTT assay of HeLa cells [35]. Briefly HeLa cells of 1×10^5cm^{-2} were seeded first onto the 96-well culture plates in DMEM media. After 24 h of incubation, fresh DMEM containing 20 μg/ ml of the samples replaced the medium in the each well and were incubated for 24, 48, and 72 h time intervals. Untreated cells grown in media were used as control. After incubation, 100 μl of MTT dye solution (0.5 mg/ml in PBS, pH 7.4) was added to each well by replacing the media containing samples and was incubated for another 4 h. 100 μl of DMSO was added in each well to dissolve the formazon crystals. The absorbance was measured at 570 nm using a micro plate reader. Cell viability was calculated by the following equation:

$$\%\text{cellviability} = \frac{\text{ODoft}}{\text{ODofc}} \times 100$$

where, c is the optical density of 'control' representing HeLa cells incubated in medium alone and t is the optical density of test specimen representing HeLa cells treated with the corresponding samples.

2.11. Fluorescence imaging

For fluorescence imaging HeLa cells were seeded in 24 well plate on cover slips as described earlier and after treated with 80 μg/mL concentration of pristine metal, ligand and metal complexes, 1×10^4cm^{-2} cells were incubated at 37 °C in CO_2 incubator. Cells on coverslips were stained with 100 μg/ml acridine orange and 100 μg/ml ethidium bromide. Then cells were incubated in dark for 30 min and were washed with PBS twice. Fluorescence microscope (Leica, Germany) captured the images.

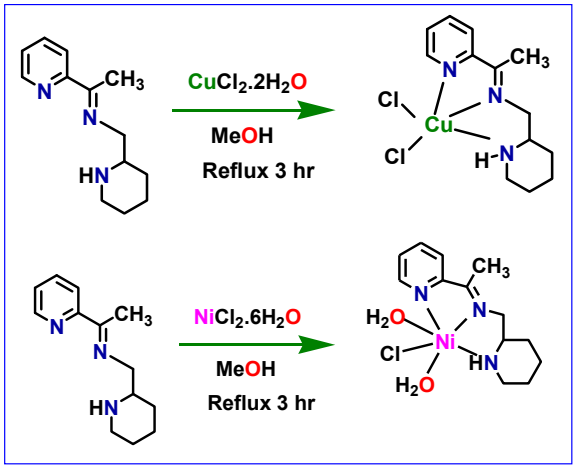

Scheme 2. Synthetic pathway for Complex (1) and (2).

3. Results and discussions

3.1. Synthesis, IR and UV–Vis analyses

The Schiff base, L obtained from the condensation reaction of 2-acyl pyridine and piperidine-2-yl-methylamine yielded complex (1) and (2) on reaction with copper (II) chloride and nickel (II) chloride respectively. The formation reaction of the complexes is shown in Scheme 2.

In the FTIR spectrum of the complex 1 (Fig. S1), a dissimilar prominent band at 1649 cm^{-1} is observed which is attributed for azomethine (C═N) group. Peaks at 3437 and 1490 cm^{-1} are characteristic peaks which are assigned for N—H stretching and bending modes respectively. C—N and C═C aromatic ring stretching frequencies are obtained at 1305 and 1666 cm^{-1} respectively. The peaks at 1203 cm^{-1} is due to C—C stretching. The other characteristic peaks at 3051, 2916 and 1340 cm^{-1} are attributed to aromatic C—H, aliphatic C—H stretching and C—H bending respectively.

In the FTIR spectrum of the complex 2 (Fig. S2), same characteristic bands were observed at the following regions: C═N: 1664 cm^{-1}, N—H stretching and bending: 3435 and 1489 cm^{-1}, C—N and C═C aromatic ring stretching: 1307 and 1664 cm^{-1}, C—C stretching: 1205 cm^{-1}, aromatic C—H, aliphatic C—H stretching and C—H bending: 3053, 2918 and 1342 cm^{-1} respectively.

In the UV–Vis spectra of the complexes, the relatively intense band at around 278–285 nm region (285 nm for complex 1 & 278 nm for complex 2) could be assigned to the π – π* transitions of aromatic rings and azomethine groups. The UV–Vis spectra of the Schiff base ligand also contained a band at around 330 nm which had been attributed to the n– π* transition, but this band was absent in the spectra of the complexes. The other bands were assigned to the charge transfer transitions between the metals and the ligands and d-d transition. The d–d bands of complexes were observed small intensities because of small molar absorption coefficient of these forbidden transitions.

3.2. Description of the structure for complex 1

The complex 1 crystallizes in the space group $P2_1/n$. Fig. 1 shows the pictorial view of the discrete mononuclear unit of it with the atom labeling scheme. In this complex, Cu(II) centre adopt square pyramidal geometry by coordinating three N atoms of L and two chlorine atoms of copper chloride. Bond parameters associated with the Cu(II) center are listed in Table S1. The Cu…..N, bond distances are in the range 1.99 – 2.03 Å which are well agreement with the literature [36–44]. The tridentate ligand forms two five membered chelate rings by coordinating to the copper via N atom of the piperidine ring (N1), the azomethine N atom (N2) and the pyridine N (N3). The two chlorine atoms (Cl1 and Cl2) are coordinated in a mutually *cis* arrangement. The basal plane around the Cu atom is formed by N1, N2, N3, Cl2 (bond lengths 1.99–2.276 Å) and the apical position is occupied by Cl1 (Cu-Cl distance 2.469 Å).

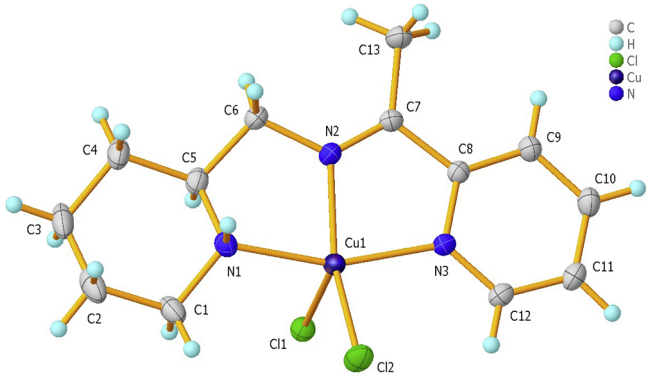

Fig. 1. ORTEP representation of the complex 1 showing 30% probability ellipsoids.

The *N*-Cu-N, *N*-Cu-Cl and Cl-Cu-Cl angular distributions indicate that the coordination polyhedron is distorted. This distortion in the Cu(II) coordination polyhedron results from steric interactions. The distortions from an ideal square pyramidal geometry occurs for the N(1)-Cu(1)-N(2) [82.16(5)°], N(1)-Cu(1)-Cl(1) [96.13(4)°], N(1)-Cu(1)-Cl(2) [96.75(4) °], Cl(2)-Cu(1)-Cl(1) [105.655(15)°], N(2)-Cu(1)-Cl(1) [104.13(4)°], N(2)-Cu(1)-Cl(2) [150.13(4)°], N(2)-Cu(1)-N(3) [78.99(5)°], N(3)-Cu(1)-Cl(1) [93.69(3)°] and N(3)-Cu(1)-Cl(2) [96.89(3)°] angles respectively. The added hydrogen bond parameters are given in Tables S3 & S4 for complex 1 and 2 respectively.

The solid-state structure of **1** includes a combination of intermolecular N—H···Cl, hydrogen bonds (Fig. 2) which finally turns the mono nuclear units to 1D polymer. The distance of N—H···Cl hydrogen bond is 2.320 Å. Besides, it is observed that in asymmetric unit the water molecule is in partial occupancy.

3.3. Description of the structure for complex 2

The space group of the complex 2 is $P2_1/c$. A pictorial view of the discrete mononuclear unit of the complex with the atom labeling scheme is shown in Fig. 3. In the complex, Ni(II) centre has an octahedral coordination. Bond parameters associated with the Ni(II) center are listed in Table S2. The tridentate ligand coordinates to the nickel via the N atom of the piperidine ring (N1A), the azomethine N atom (N2) and the pyridine N (N3), forming two five membered chelate rings. The two oxygen atoms (O1L and O2L) are coordinated in a mutually *trans* arrangement and one chlorine atom (Cl1L) is also coordinated to the nickel.

The bond lengths of the metal to the Schiff base (NNN donor) are, Ni1–N1A = 2.106(6) Å, Ni1–N2 = 2.017(2) Å and Ni1–N3 = 2.090(2)

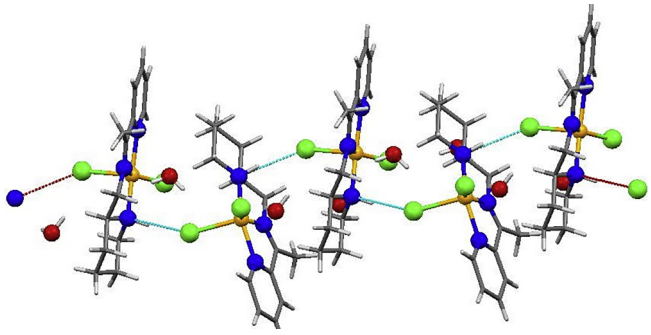

Fig. 2. 1D polymer structure of complex 1.

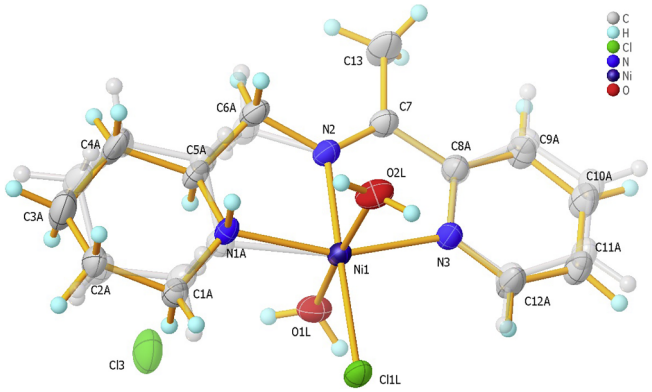

Fig. 3. ORTEP representation of the complex 2 showing 50% probability ellipsoids.

Å. In the complex 2, the Ni(II) center has a distorted octahedral coordination. Due to this elongated octahedral coordination environment of the metal center, two five-membered chelate rings were formed. The angular distributions [N–Ni–N, N–Ni–O and N–Ni–Cl] indicate the distortion around the coordination polyhedra. The distortion of the coordination polyhedron around the Ni(II) ion arises due to the steric interactions in which the maximum distortion from an ideal octahedral geometry occurs for the N(1A)–Ni(1)–O(1L) [98.25(16)°], O(1L)- Ni(1)-Cl(1L) [91.32(6)°], O(1L)-Ni(1)-O(2L) [173.93(9)°], O(2L)-Ni(1)-Cl(1L) [91.57(6)°], O(2L)-Ni(1)-N(1A) [86.53(16)°], N(2)-Ni(1)-Cl(1L) [178.61(7)°], N(2)-Ni(1)-O(1L) [88.68(9)°], N(2)-Ni(1)-O(2L) [88.31(9)°] and N(2)–Ni(1)–N(3) [78.50(9)°] angles.

Actually, the structure of complex 2 which is represented in Fig. 3 is disordered in a ratio of 55/45. The major part (labeled A) is shown in the figure as 'solid' while the minor part is shown as a transparent 'ghost' image. The disorder is 'whole ligand' disorder, where one ligand is in the 'up' position, and the other one in the 'down' position. ORTEP representation of the complex 2 (Fig. 3) showed 50% probability ellipsoids of the structure.

Besides, each mono nuclear unit of complex (2) forms a 1D chain (Fig. 4) via O—H…Cl hydrogen bond. The O_{2L}-H_{2LA}…Cl (3) distance is 2.251 Å and that for O_{1L}-H_{1LA}…Cl (3) distance is 2.259 Å which are in accordance with reported distance [45–48]. It is also noticed that these two parallel chain further hydrogen bonded through O—H…Cl having O_{2L}-H_{2L}…Cl (1L) and O_{1L}-H_{1LB}…Cl(1L) distances are respectively 2.312 and 2.328 Å and thus form a ladder like 1D polymer (Fig. 4).

3.4. Antibacterial activity

Antibacterial activity was studied using the bacterial strain E. coli using Agar media (broth). To 30 ml of broth, 100 µl of bacteria was added and incubated for 24 h. The next day turbidity in Petridis indicated bacterial growth [49]. Now treatment was done by adding metal, ligand and their complexes (50 µl) in each Petridis and incubated at 37 ^{O}C for overnight (Figure S3). It was found from the figure that turbidity appeared for metal salt $CuCl_2$ and complex 1. Since turbidity in petridish after treatment indicates bacterial growth and clarity denoted inhibition of bacterial growth so from the result it is clear that among metals only $CuCl_2$ and among complexes only complex 1 exhibited anti bacterial property.

3.5. DNA binding studies

3.5.1. UV–vis absorption titration and binding affinity evaluation

The binding interaction has been speculated by the absorption titration of complexes **1** & **2** with CT-DNA. The bands at 260 and 280 nm observed in the spectrum of CT-DNA in the buffer authenticate that the DNA is adequately free from protein [50]. The binding affinity of complexes **1** & **2** with CT-DNA has been determined at constant complex concentration and with regular addition of CT-DNA. The absorption titration of the complex **1** & **2** with the increase in the concentration of CT-DNA has been represented by Fig. 5. The figure represents that complex **1** & **2** shows maxima at 642 and 807 nm respectively which on addition of CT-DNA gradually decrease with a hypsochromism along with a blue shift for both. An interesting observation is that absorption band splits into two new shoulder (at 682 and 596 nm for complex **1** & 831 and 727 nm for complex **2**) on gradual addition of CT-DNA into complex (**1** & **2**) solution with continuous decrement up to saturation. This observation suggested a strong interaction between complex and DNA as well as generation of a new species upon interaction. The presence of isosbestic points at 523 nm (complex **1**) and 658 nm (complex **2**) clearly indicates a strong reversible equilibrium external binding occurred in presence of CT-DNA. Experimental results revealed the intercalating binding nature for $\pi \rightarrow \pi^*$ stacking interactions between the base pairs of CT-DNA and complex **1** & **2** [51,52]. However, absorption titration is not able to give the quantitative mode of binding. The calculated binding constant (K_b) is acquired from the ratio of the slope to the y-intercept in plots ([DNA])/ ($\varepsilon_A - \varepsilon_f$) versus [DNA] according to equation (1). Fig. 5 represents the best fit of the experimental value to equation (1). The binding affinity (K_b) obtained from this titration experiment was 8.1×10^5 M^{-1} (for complex **2)** and 9×10^5 M^{-1} (for complex **1**). These confirmed that the complex bind to CT- DNA quite strongly. The binding constant values obtained from this experiment are very much comparable with the reported other Cu and Ni complexes [53–58]. The calculated DNA binding affinity of complex **2** is slightly higher than that complex **1**.

3.5.2. Ethidium bromide (EB) displacement studies

EB displacement studies were performed to speculate further insights of the binding behavior between CT-DNA and complex **1** & **2**. EB,

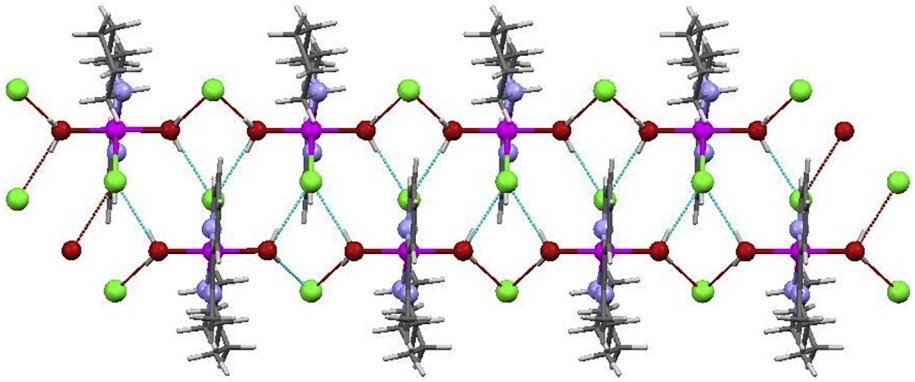

Fig. 4. 1D polymer structure of complex 2.

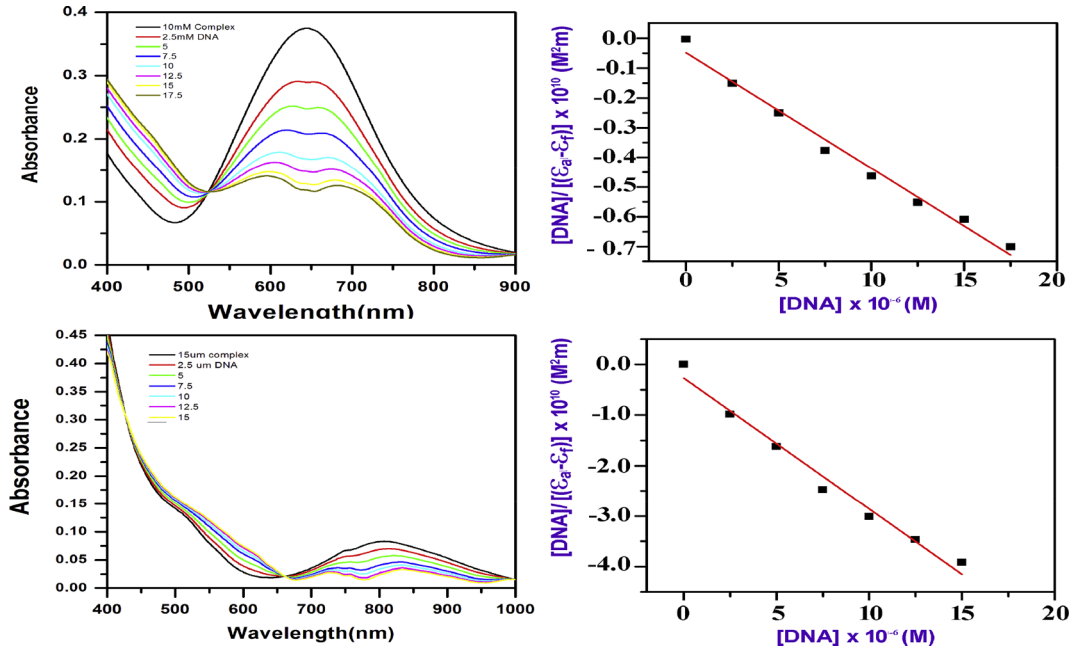

Fig. 5. UV–Vis absorption spectra of complexes **1** and **2** upon the addition of CT-DNA ([complex **1**] = 10 μM ; [CT-DNA] = 2.5 to 17.5 μM for complex **1** and [complex **2**] = 15 μM; [CT-DNA] = 2.5 to 15 μM for complex **2**). *Inset* plot of [DNA]/($\varepsilon_a - \varepsilon_f$) versus [DNA] for the titration of DNA to complexes.

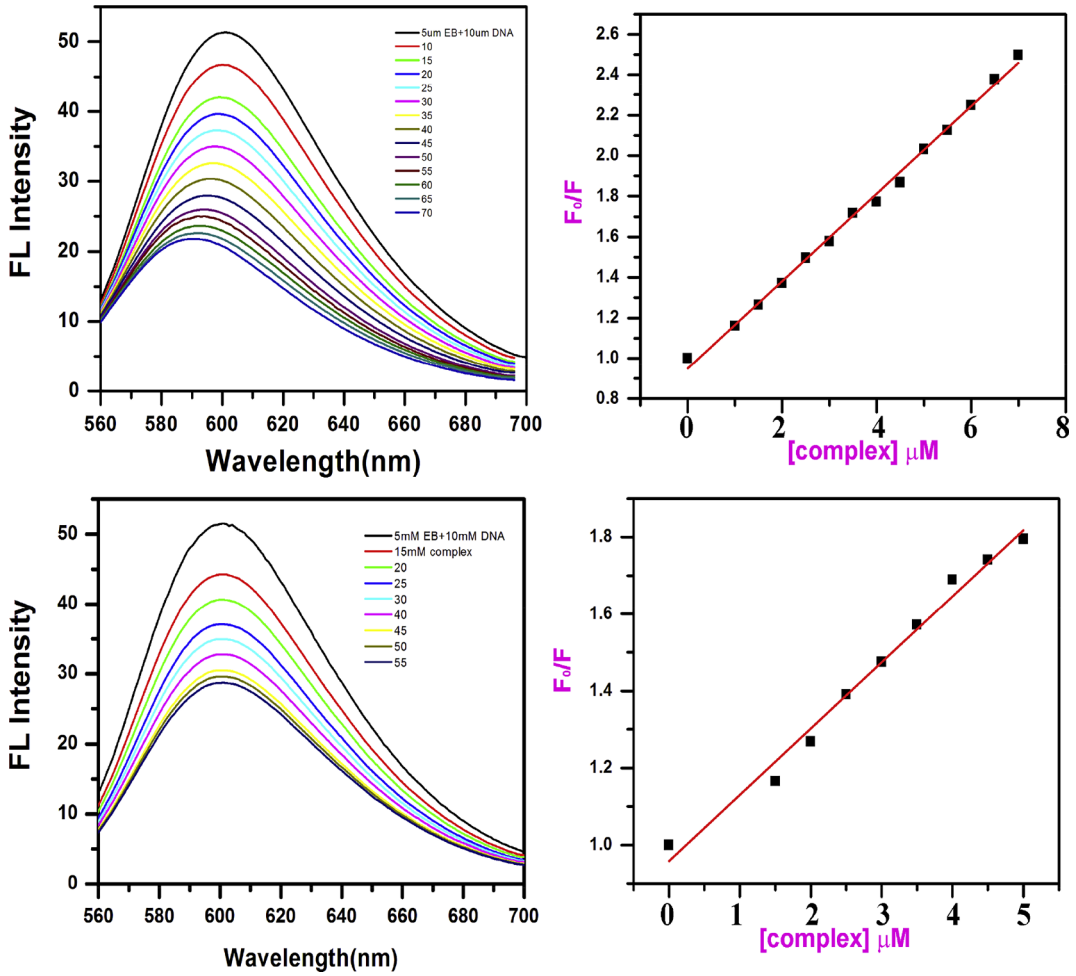

Fig. 6. Effect of the addition of complexes **1** and **2** on the emission intensity of the CT-DNA bound EB at different concentrations ([EB] = [CT-DNA] = 5 μM; [Complex **1**] = 0–70 μM, [Complex **2**] = 0–55 μM. Stern–Volmer plot of the fluorescence data.

a phenanthiridine fluorescence dye, is a typical example of intercalator because in a single probe it shows very weak fluorescence but on incorporation of CT–DNA in it a large enhancement was observed. This is because of the fact that planar phenanthiridine ring is perfectly fitted in to the adjacent base pairs of the double helix [59]. A notable decrease in emission intensities (Fig. 6) is observed upon increase in the concentration of complex **1** & **2** to the EB-CT-DNA system. It is due to the intercalation of Cu and Ni complexes to DNA base pairs. During this process some EB molecules have been replaced from the EB–CT-DNA system i.e. the decrease in fluorescence intensity was observed due to the reduction of the number of binding sites on the CT-DNA available to the EB. Quenching parameters were analyzed following the Stern−-Volmer equation.

$$\frac{F^0}{F} = K_{SV}[Q] + 1$$

where F^0 is the emission intensity in the absence of the compound, F is the emission intensity in the presence of the compound, K_{SV} is the quenching constant, and [Q] is the concentration of the compound. The K_{SV} value is obtained as a slope from the plot of F^0/F versus [Q]. The quenching constant (K_{sv}) obtained for complex **1** & **2** are 1.73×10^5 and 2.3×10^5 respectively.

With the help of the following equation the apparent DNA binding constant (K_{app}) values were also calculated

$$K_{EB}[EB] = K_{app}[complex]$$

where [complex] is the value at 50% decrease in the fluorescence intensity of CT-DNA- EB complex, K_{EB} ($1.22 \pm 0.72 \times 10^7$ $M^{-1}$and [EB] = 5 μM) is the DNA binding constant of EB. The K_{app} values for the complex were found to be 0.87×10^6 M^{-1} (for complex **1**) and 1.24×10^6 M^{-1} (for complex 2). The observed quenching and binding parameters conclude that the complex bind DNA via intercalation mode [54–57,59].

3.5.3. Viscosity measurements

Since viscosity changes are sensitive to the increase in length so viscosity measurement has been performed on getting the indication of intercalation mode from the ethidium bromide (EB) displacement study. Generally in intercalation mode insertion of the compound between the base pair increases the length of DNA and thereby increases viscosity [60]. On the other hand, groove, stacking and non-classic intercalation binding result in a twist or bend in the DNA helix and cause slightly reduce its actual length. So in this case viscosity is either slightly decreased or remains in unchanged [61–64]. Fig. 7 shows the relative viscosity of CT-DNA-EB and CT-DNA- complex 1 & 2 solutions

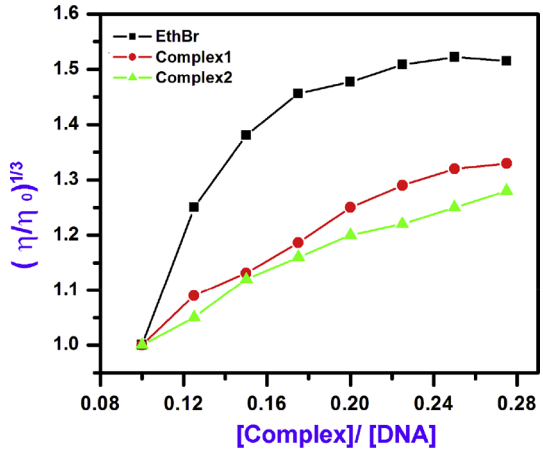

Fig. 7. Effects of increasing concentration of ethidium bromide (EB). Effect of increasing amounts of Complex **1** and complex **2** on the relative specific viscosity of Calf Thymus DNA (CT-DNA = 2 mM).

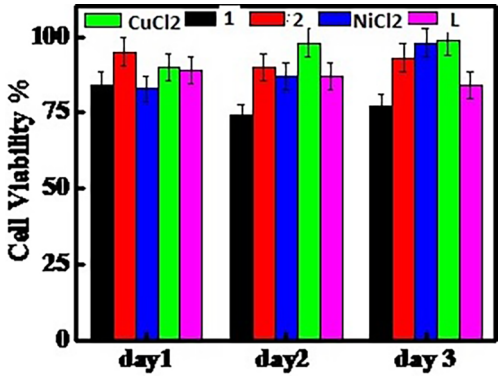

Fig. 8. Cell viability of Hela cells on metal ($CuCl_2$, $NiCl_2$), ligand L and Complexes 1 & 2.

with the increasing amount of EB/complex. A slight increase in the relative viscosity of CT-DNA is observed on the addition of complex (0.1–0.28 mM) which indicates that insertion of complex between the CT-DNA base pair results in lengthening the original size of DNA. However, it is clear from the comparison study with EB that the change in relative viscosity during the interaction is very much smaller than the EB (a classical intercalator). So it can be concluded that binding mode is not fully intercalation rather it is a partial intercalation [34,65].

3.5.4. Cell viability

The present study also emphasized on cell viability analyses. For that, MTT assay has been used to check cell viability of Hela cells on metal, ligand and its corresponding complexes 1 & 2. The results are represented in Fig. 8. It is observed from figure that cell viability increases with time for all the systems i.e metals, ligands and their complexes illustrating their biocompatible nature. It is also clear that among the complexes 1 and 2, complex 1 shows higher cell viability. The biocompatible nature is also evident from cell morphology obtained through fluorescence images of Hela cells of metal complexes after staining with acridine orange and ethidium bromide dye [66] (Figs. 9 & 11). It is worth mentioning here that cell health as well as number density of cells is better that means the metal complexes are biocompatible in nature.

Another technique i.e. adhesion behavior of Hela cells on pure metal, ligand and its complexes is also used to check biocompatibility of the said compounds. It was clearly observed that cells were adhered properly on both the metal complexes 1 & 2 as compared to pure metal and ligand. This observation further demonstrates their biocompatibility indicating their uses as biomaterial transplants (Figs. 10 & 12).

4. Conclusions

The present paper discusses the synthesis and characterization of new Cu(II) and Ni(II) complexes of a tridentate NNN Schiff base ligand which is readily synthesized from the Schiff reaction of an aldehyde and amine. In the complexes, Cu(II) occupies square pyramidal coordination and Ni(II) center occupies octahedral coordination. The backbone of the net supramolecular arrangement dictated by hydrogen bonds has been constituted by the primary structural motifs which are revealed from the MOFs in the title complexes. From the antibacterial screening it is shown that among metals only $CuCl_2$ and among complexes only complex 1 exhibited anti bacterial property. DNA interactions with the complexes have been investigated by a range of experimental techniques that express the partial intercalation mode of DNA binding with the complexes. From cell viability test it is observed that all the systems i.e. metals, ligands and their complexes are biocompatible in nature since cell viability increases with time. Among the complexes 1 and 2, complex 1 shows higher cell viability. It was also clearly observed that

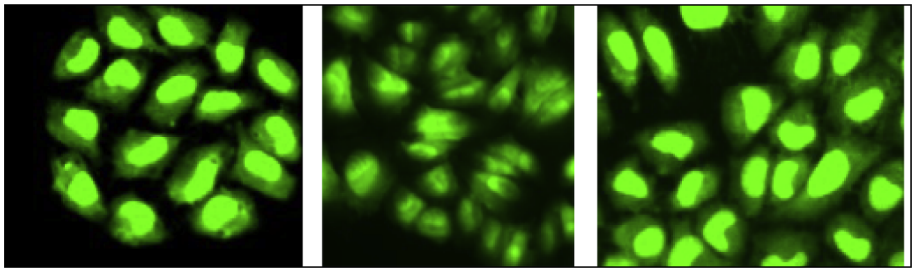

Fig. 9. Fluorescent images of AO/EB staining of (a) $CuCl_2$, (b) L and (c) Complex 1.

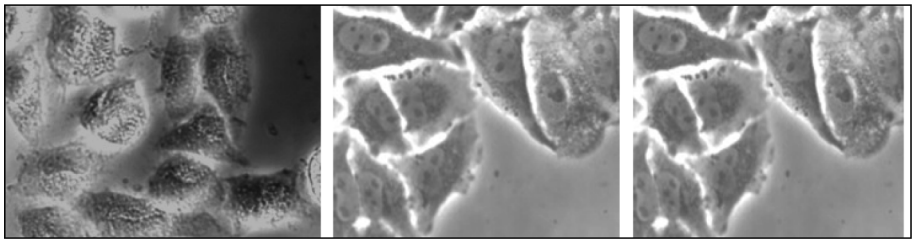

Fig. 10. Cell adhesion images (a) $CuCl_2$, (b) L and (c) Complex 1.

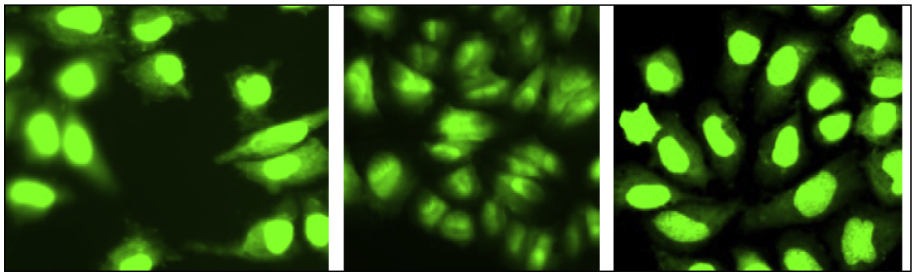

Fig. 11. Fluorescent images of AO/EB staining of (a) $NiCl_2$, (b) L and (c) Complex 2.

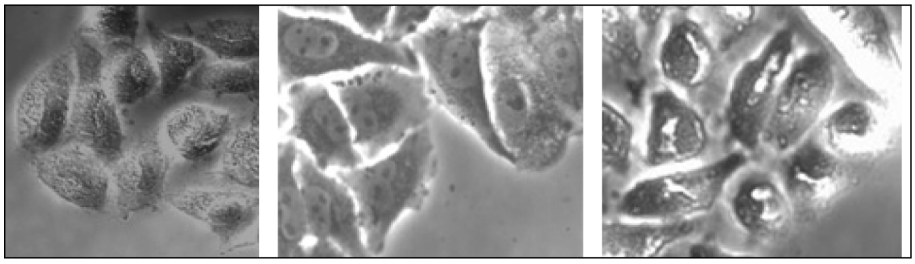

Fig. 12. Cell adhesion images (a) $NiCl_2$, (b) L and (c) Complex 2.

cells were adhered properly on both the metal complexes 1 & 2 as compared to pure metal and ligand. This observation again demonstrates it biocompatibility indicating its use as a biomaterial transplant. Further studies on the antioxidant, antifungal as well as DNA cleavage studies, are planned for the future.

Conflicts of interest

There are no conflicts to declare.

Acknowledgements

Authors acknowledge the financial support from the University Grants Commission, Eastern Regional Office through Minor Research Project [No. F. PSW-131/13-14 (ERO) dated 18-Mar-14]. Somnath Das gratefully acknowledges the University Grants Commission (UGC) (award letter number: 2061610244/19-06-2016), Govt. of India, New Delhi for the award of Junior Research Fellowship (JRF). Authors thank Dr. Debaprasad Mandal's group (Dept. of Chemistry, IIT, Ropar) for providing FTIR spectra and also wish to thank Prof. Pralay Maiti's group, School of Materials Science and Technology, Indian Institute of Technology (BHU), Varanasi for antibacterial and cell viability tests. KJ and TM are thankful to University Grants Commission.

Appendix A. Supplementary data

Supplementary data to this article can be found online at https://doi.org/10.1016/j.ica.2018.12.007.

References

[1] M.M. Mostafa, K.M. Ibrahim, M.N.H. Moussa, Bivalent metal complexes ofp-methyl-andp-methoxybenzoylhydrazone oximes, Transition Met. Chem. 9 (1984) 243–246.
[2] A. Shanmugapriya, G. Kalaiarasi, P. Kalaivani, F. Dallemer, R. Prabhakaran, CT-DNA/BSA protein binding and antioxidant studies of new binuclear Pd(II) complexes and their structural characterisation, Inorg. Chim. Acta 449 (2016) 107–118.
[3] H. Wu, F. Kou, F. Jia, B. Liu, J. Yuan, Y. Bai, A V-shaped ligand 1,3-bis(1-

methylbenzimidazol-2-yl)-2-oxapropane and its Cu(II) complex: Synthesis, crystal structure, antioxidation and DNA-binding properties, J. Photochem. Photobiol., B 105 (2011) 190–197.
[4] B.K. Rai, P. Choudhary, P. Sahi, S. Rana, Synthesis, characterization and antifungal studies of some Schiff base complexes of Co(II), Ni(II) and Cu(II) with 6-bromo 2-thio-3-phenyl quinazoline-4 (3H) one semicarbazone, Orient J Chem 23 (2007).
[5] M. Salehi, M. Hasanzadeh, Characterization, crystal structures, electrochemical and antibacterial studies of four new binuclear cobalt(III) complexes derived from o-aminobenzyl alcohol, Inorg. Chim. Acta 426 (2015) 6–14.
[6] S.A. Patil, S.N. Unki, A.D. Kulkarni, V.H. Naik, P.S. Badami, Synthesis, characterization, in vitro antimicrobial and DNA cleavage studies of Co(II), Ni(II) and Cu(II) complexes with ONOO donor coumarin Schiff bases, J. Mol. Struct. 985 (2011) 330–338.
[7] A.Z. El-Sonbati, A.A. El-Bindary, E.M. Mabrouk, Synthesis and physico-chemical studies on transition metal complexes of symmetric bis-Schiff base ligands, Transition Met. Chem. 17 (1992) 66–70.
[8] R.F.M. Elshaarawy, Z.H. Kheiralla, A.A. Rushdy, C. Janiak, New water soluble bis-imidazolium salts with a saldach scaffold: synthesis, characterization and in vitro cytotoxicity/bactericidal studies, Inorg. Chim. Acta 421 (2014) 110–122.
[9] T. Opstal, F. Verpoort, Ruthenium indeny- lidene and vinylidene complexes bearing Schiff bases: potential catalysts in Enol – Ester Synthesis, Synlett 6 (2002) 935–941.
[10] S. Pal, S. Pal, A Diruthenum(III) Complex Possessing a Diazine and Two Chloride Bridges: Synthesis, Structure, and Properties, Inorganic Chem. 40 (2001) 4807–4810.
[11] G. Romanowski, T. Lis, Chiral oxidovanadium(V) complexes with tridentate Schiff bases derived from S(+)-2-amino-1-propanol: Synthesis, structure, characterization and catalytic activity, Inorg. Chim. Acta 394 (2013) 627–634.
[12] A. Garoufis, S.K. Hadjikakou, N. Hadjiliadis, Palladium coordination compounds as anti-viral, anti-fungal, anti-microbial and anti-tumor agents, Coord. Chem. Rev. 253 (2009) 1384–1397.
[13] Y.-L. Zhang, W.-J. Ruan, X.-J. Zhao, H.-G. Wang, Z.-A. Zhu, Synthesis and characterization of axial coordination cobalt(III) complexes containing chiral Salen ligands, Polyhedron 22 (2003) 1535–1545.
[14] Y. Zhu, W. Li, Syntheses, crystal structures and antibacterial activities of azido-bridged cobalt(III) complexes with Schiff bases, Transition Metal Chem. 35 (2010) 745–749.
[15] G.R. Desiraju, T. Steiner, The Weak Hydrogen Bond in Structural Chemistry and Biology, in, Oxford University Press, Oxford, 1999.
[16] A. Frontera, M. Orell, C. Garau, D. Quiñonero, E. Molins, I. Mata, J. Morey, Preparation, Solid-State Characterization, and Computational Study of a Crown Ether Attached to a Squaramide, Org. Lett. 7 (2005) 1437–1440.
[17] M. Nishio, M. Hirota, Y. Umezawa, The CH/π Interaction: Evidence, Nature, and Consequences, in, 1998, p. 232.
[18] M. Nishio, Y. Umezawa, K. Honda, S. Tsuboyama, H. Suezawa, CH/[small pi] hydrogen bonds in organic and organometallic chemistry, CrystEngComm 11 (2009) 1757–1788.
[19] Y. Zhang, Z. Yang, F. Yuan, H. Gu, P. Gao, B. Xu, Molecular Recognition Remolds the Self-Assembly of Hydrogelators and Increases the Elasticity of the Hydrogel by 106-Fold, J. Am. Chem. Soc. 126 (2004) 15028–15029.
[20] M.J. Packer, M.P. Dauncey, C.A. Hunter, Sequence-dependent DNA structure: dinucleotide conformational maps11Edited by A Klug, J. Mol. Biol. 295 (2000) 71–83.
[21] J.K. Barton, Metals and DNA: molecular left-handed complements, Science 233 (1986) 727.
[22] K.E. Erkkila, D.T. Odom, J.K. Barton, Recognition and Reaction of Metallointercalators with DNA, Chem. Rev. 99 (1999) 2777–2796.
[23] L.-N. Ji, X.-H. Zou, J.-G. Liu, Shape- and enantioselective interaction of Ru(II)/Co(III) polypyridyl complexes with DNA, Coord. Chem. Rev. 216–217 (2001) 513–536.
[24] J. Mann, A. Baron, Y. Opoku-Boahen, E. Johansson, G. Parkinson, L.R. Kelland, S. Neidle, A New Class of Symmetric Bisbenzimidazole-Based DNA Minor Groove-Binding Agents Showing Antitumor Activity, J. Med. Chem. 44 (2001) 138–144.
[25] A. Meenongwa, R.F. Brissos, C. Soikum, P. Chaveerach, P. Gamez, Y. Trongpanich, U. Chaveerach, DNA-interacting and biological properties of copper(ii) complexes from amidino-O-methylurea, New J. Chem. 39 (2015) 664–675.
[26] O.V. Dolomanov, L.J. Bourhis, R.J. Gildea, J.A.K. Howard, H. Puschmann, OLEX2: a complete structure solution, refinement and analysis program, J. Appl. Crystallogr. 42 (2009) 339–341.
[27] L. Palatinus, G. Chapuis, SUPERFLIP—A Computer Program for the Solution of Crystal Structures by Charge Flipping in Arbitrary Dimensions, J. Appl. Crystallogr. 40 (2007) 786–790.
[28] L.J. Bourhis, O.V. Dolomanov, R.J. Gildea, J.A.K. Howard, H. Puschmann, The anatomy of a comprehensive constrained, restrained refinement program for the modern computing environment - Olex2 dissected, Acta Crystallographica Section A 71 (2015) 59–75.
[29] S. Belghith, Y. Bahrouni, L.B. Hamada, Synthesis, Crystal Structure and Characterization of a New Dihydrogenomonophosphate: (C7H9N2O)H2PO4, Open J. Inorganic Chem. 5 (2015).
[30] C. Perez, M. Pauli, P. Bazerque, An Antibiotic Assay by Agar Well Diffusion Method, Acta Biologiaeet Medicinae Experimentalis 15 (1990) 113–115.
[31] A. Wolfe, G.J. Shimer, T. Meehan, Polycyclic aromatic hydrocarbons physically intercalate into duplex regions of denatured DNA, Biochemistry 26 (1987) 6392–6396.
[32] V. Rajendiran, R. Karthik, M. Palaniandavar, V.S. Periasamy, M.A. Akbarsha, B.S. Srinag, H. Krishnamurthy, Mixed-Ligand Copper(II)-phenolate Complexes: Effect of Coligand on Enhanced DNA and Protein Binding, DNA Cleavage, and Anticancer Activity, Inorganic Chem. 46 (2007) 8208–8221.
[33] F. Dimiza, A.N. Papadopoulos, V. Tangoulis, V. Psycharis, C.P. Raptopoulou, D.P. Kessissoglou, G. Psomas, Biological evaluation of non-steroidal anti-inflammatory drugs-cobalt(ii) complexes, Dalton Trans. 39 (2010) 4517–4528.
[34] A. Tarushi, E. Polatoglou, J. Kljun, I. Turel, G. Psomas, D.P. Kessissoglou, Interaction of Zn(ii) with quinolone drugs: structure and biological evaluation, Dalton Trans. 40 (2011) 9461–9473.
[35] S. Senapati, R. Thakur, S.P. Verma, S. Duggal, D.P. Mishra, P. Das, T. Shripathi, M. Kumar, D. Rana, P. Maiti, Layered double hydroxides as effective carrier for anticancer drugs and tailoring of release rate through interlayer anions, J. Control. Release 224 (2016) 186–198.
[36] H. Karabıyık, Ö. Erdem, M. Aygün, B. Güzel, S. García-Granda, Ligand-to-Metal Charge Transfer Resulting in Metalloaromaticity of [R, R-Cyclohexyl-1,2-bis(2-Oxidonaphthylideneiminato-N, N′, O, O′)]Cu(II): A Scrutinized Structural Investigation, J. Inorg. Organomet. Polym Mater. 20 (2010) 142–151.
[37] A.D. Khalaji, M. Gholinejad, S. Triki, The copper(II) complexes with tetradentate Schiff base ligands: synthesis, crystal structures, and computational studies, Russ. J. Coord. Chem. 39 (2013) 209–213.
[38] L. Mouni, M. Akkurt, S.Ö. Yıldırım, T.B. Hadda, Z.H. Chohan, Crystal Structure of Cuprate (II) Complex of Tetradentate ONNO Ligand: 4-[(2-{[(1E)-1-Methyl-3-oxobutylidene]amino}ethyl)imino]pentan-2-one, J. Chem. Crystallogr. 40 (2010) 169–172.
[39] P. Mukherjee, M.G.B. Drew, A. Figuerola, A. Ghosh, Incorporation of a sodium ion guest in the host of copper(II)-Schiff-base complexes: Structural characterization and magnetic study, Polyhedron 27 (2008) 3343–3350.
[40] L.C. Nathan, J.E. Koehne, J.M. Gilmore, K.A. Hannibal, W.E. Dewhirst, T.D. Mai, The X-ray structures of a series of copper(II) complexes with tetradentate Schiff base ligands derived from salicylaldehyde and polymethylenediamines of varying chain length, Polyhedron 22 (2003) 887–894.
[41] M. Ulusoy, H. Karabıyık, R. Kılınçarslan, M. Aygün, B. Çetinkaya, S. García-Granda, Co(II) and Cu(II) Schiff base complexes of bis(N-(4-diethylamino-2-methylphenyl)-3,5-di-tert-butylsalicylaldimine): electrochemical and X-ray structural study, Struct. Chem. 19 (2008) 749–755.
[42] P.A.N. Reddy, B.K. Santra, M. Nethaji, A.R. Chakravarty, Metal-assisted light-induced DNA cleavage activity of 2-(methylthio)phenylsalicylaldimine Schiff base copper(II) complexes having planar heterocyclic bases, J. Inorg. Biochem. 98 (2004) 377–386.
[43] P. Talukder, A. Datta, S. Mitra, G. Rosair, Square Planar Complexes of Cu(II) with an N2O Donor Set of a New Schiff Base Ligand: Synthesis and Structural Aspects, Zeitschrift für Naturforschung B (2004) 655.
[44] F. Tuna, L. Patron, Y. Journaux, M. Andruh, W. Plass, J.-C. Trombe, Synthesis and magnetic properties of a series of bi- and tri-nuclear complexes of copper(II) with the unsymmetrical tetradentate Schiff-base ligand 3-[N-2-(pyridylethyl)formimidoyl]salicylic acid, H2fsaaep, and crystal structures of [{Cu(Hfsaaep)Cl}2] and [{Cu(fsaaep)(H2O)}2], J. Chem. Soc. Dalton Trans. (1999) 539–546.
[45] M. Amirnasr, K.J. Schenk, M. Salavati, S. Dehghanpour, A. Taeb, A. Tadjarodi, Synthesis and Characterization of Cobalt(II), Nickel(II), and Zinc(II) Complexes with N, N ′-bis(Trans- Cinnamaldehyde)-1,2-Diiminoethane Ligand, (ca 2 en): Crystal and Molecular Structures of Co(ca 2 en)Cl 2, Co(ca 2 en)Br 2 and Ni(ca 2 en) Br 2, J. Coord. Chem. 56 (2003) 231–243.
[46] M.R. Hasan, M.A. Hossain, M.A. Salam, M.N. Uddin, Nickel complexes of Schiff bases derived from mono/diketone with anthranilic acid: Synthesis, characterization and microbial evaluation, J. Taibah Univ. Sci. 10 (2016) 766–773.
[47] A. Majumder, G.M. Rosair, A. Mallick, N. Chattopadhyay, S. Mitra, Synthesis, structures and fluorescence of nickel, zinc and cadmium complexes with the N, N, O-tridentate Schiff base N-2-pyridylmethylidene-2- hydroxy-phenylamine, Polyhedron 25 (2006) 1753–1762.
[48] P. Mukherjee, M.G.B. Drew, C.J. Gómez-García, A. Ghosh, The Crucial Role of Polyatomic Anions in Molecular Architecture: Structural And Magnetic Versatility of Five Nickel(II) Complexes Derived from A N, N, O-Donor Schiff Base Ligand, Inorganic Chem. 48 (2009) 5848–5860.
[49] A.K. Mahanta, S. Senapati, P. Maiti, A polyurethane-chitosan brush as an injectable hydrogel for controlled drug delivery and tissue engineering, Polym. Chem. 8 (2017) 6233–6249.
[50] N. Raman, R. Jeyamurugan, M. Subbulakshmi, R. Boominathan, C.R. Yuvarajan, Synthesis, DNA binding, and antimicrobial studies of novel metal complexes containing a pyrazolone derivative Schiff base, Chem. Pap. 64 (2010) 318–328.
[51] S. Jain, T.A. Khan, Y.P. Patil, D. Pagariya, N. Kishore, S. Tapryal, A.D. Naik, S.G. Naik, Bio-affinity of copper(II) complexes with nitrogen and oxygen donor ligands: Synthesis, structural studies and in vitro DNA and HSA interaction of copper (II) complexes, J. Photochem. Photobiol., B 174 (2017) 35–43.
[52] K. Tishchenko, E. Beloglazkina, M. Proskurnin, V. Malinnikov, D. Guk, M. Muratova, O. Krasnovskaya, A. Udina, D. Skvortsov, R.R. Shafikov, Y. Ivanenkov, V. Aladinskiy, I. Sorokin, O. Gromov, A. Majouga, N. Zyk, New copper(II) thiohydantoin complexes: Synthesis, characterization, and assessment of their interaction with bovine serum albumin and DNA, J. Inorg. Biochem. 175 (2017) 190–197.
[53] L.H. Abdel-Rahman, A.M. Abu-Dief, R.M. El-Khatib, S.M. Abdel-Fatah, Sonochemical synthesis, DNA binding, antimicrobial evaluation and in vitro anticancer activity of three new nano-sized Cu(II), Co(II) and Ni(II) chelates based on tri-dentate NOO imine ligands as precursors for metal oxides, J. Photochem. Photobiol., B 162 (2016) 298–308.
[54] J. Lakshmipraba, S. Arunachalam, A. Riyasdeen, R. Dhivya, M.A. Akbarsha, Polyethyleneimine anchored copper(II) complexes: synthesis, characterization, in vitro DNA binding studies and cytotoxicity studies, J. Photochem. Photobiol., B 142 (2015) 59–67.

[55] Y. Manojkumar, S. Ambika, R. Senthilkumar, S. Arunachalam, Biophysical and biological studies of some polymer grafted metallo-intercalators, Colloids Surf., B 156 (2017) 320–329.
[56] P. Nithya, S. Helena, J. Simpson, M. Ilanchelian, A. Muthusankar, S. Govindarajan, New cobalt(II) and nickel(II) complexes of benzyl carbazate Schiff bases: Syntheses, crystal structures, in vitro DNA and HSA binding studies, J. Photochem. Photobiol., B 165 (2016) 220–231.
[57] H. Ünver, B. Boyacıoğlu, C.T. Zeyrek, M. Yıldız, N. Demir, N. Yıldırım, O. Karaosmanoğlu, H. Sivas, A. Elmalı, Synthesis, spectral and quantum chemical studies and use of (E)-3-[(3,5-bis(trifluoromethyl)phenylimino)methyl]benzene-1,2-diol and its Ni(II) and Cu(II) complexes as an anion sensor, DNA binding, DNA cleavage, anti-microbial, anti-mutagenic and anti-cancer agent, J. Mol. Struct. 1125 (2016) 162–176.
[58] Q. Wei, J. Dong, P. Zhao, M. Li, F. Cheng, J. Kong, L. Li, DNA binding, BSA interaction and SOD activity of two new nickel(II) complexes with glutamine Schiff base ligands, J. Photochem. Photobiol., B 161 (2016) 355–367.
[59] V.A. Izumrudov, M.V. Zhiryakova, A.A. Goulko, Ethidium Bromide as a Promising Probe for Studying DNA Interaction with Cationic Amphiphiles and Stability of the Resulting Complexes, Langmuir 18 (2002) 10348–10356.
[60] S. Satyanarayana, J.C. Dabrowiak, J.B. Chaires, Neither.DELTA.- nor.LAMBDA.-tris (phenanthroline)ruthenium(II) binds to DNA by classical intercalation, Biochemistry 31 (1992) 9319–9324.
[61] E. Chalkidou, F. Perdih, I. Turel, D.P. Kessissoglou, G. Psomas, Copper(II) complexes with antimicrobial drug flumequine: Structure and biological evaluation, J. Inorg. Biochem. 113 (2012) 55–65.
[62] J.L. García-Giménez, G. Alzuet, M. González-Álvarez, M. Liu-González, A. Castiñeiras, J. Borrás, Oxidative nuclease activity of ferromagnetically coupled μ-hydroxo-μ-propionato copper(II) complexes [Cu3(L)2(μ-OH)2(μ-propionato)2] L = N-(pyrid-2-ylmethyl)R-sulfonamidato, R = benzene, toluene, naphthalene, J. Inorg. Biochem. 103 (2009) 243–255.
[63] D.-D. Li, J.-L. Tian, W. Gu, X. Liu, S.-P. Yan, A novel 1,2,4-triazole-based copper(II) complex: synthesis, characterization, magnetic property and nuclease activity, J. Inorg. Biochem. 104 (2010) 171–179.
[64] E. Ramachandran, D. Senthil Raja, N.P. Rath, K. Natarajan, Role of Substitution at Terminal Nitrogen of 2-Oxo-1,2-dihydroquinoline-3-Carbaldehyde Thiosemicarbazones on the Coordination Behavior and Structure and Biological Properties of Their Palladium(II) Complexes, Inorg. Chem. 52 (2013) 1504–1514.
[65] A. Tarushi, C.P. Raptopoulou, V. Psycharis, A. Terzis, G. Psomas, D.P. Kessissoglou, Zinc(II) complexes of the second-generation quinolone antibacterial drug enrofloxacin: Structure and DNA or albumin interaction, Bioorg. Med. Chem. 18 (2010) 2678–2685.
[66] D.K. Patel, S. Senapati, P. Mourya, M.M. Singh, V.K. Aswal, B. Ray, P. Maiti, Functionalized Graphene Tagged Polyurethanes for Corrosion Inhibitor and Sustained Drug Delivery, ACS Biomater. Sci. Eng. 3 (2017) 3351–3363.